Asian Journal of Chemistry; Vol. 35, No. 7 (2023), 1707-1713

ASIAN JOURNAL OF CHEMISTRY

https://doi.org/10.14233/ajchem.2023.27952

Structural, Optical, Electrical and Discharge Characteristics of PVA-ZnS Nanocomposite Polymer Electrolyte–Zn^{2+} Ion Conduction for Solid State Battery Applications

R. VENUGOPAL[1,2,*], K. SUDHAKAR[1], N. NARSIMLU[1] and CH. SRINIVAS[1]

[1]Department of Physics, University College of Science, Osmania University, Hyderabad-500007, India
[2]Department of Physics, Government Degree College, Mahabubabad-506101, India

*Corresponding author: E-mail: venumrc.iisc@gmail.com

Received: 30 April 2023; *Accepted*: 7 June 2023; *Published online*: 6 July 2023; AJC-21296

Polyvinyl alcohol (PVA) based Zn^{2+} ion conducting solid polymer electrolyte was prepared using a solution-cast method. Measurements were taken utilizing X-ray diffraction (XRD) and Fourier transform infrared analysis (FT-IR) to investigate the structure. The optical absorption spectra were investigated in the 200-800 nm range in order to acquire information about the optical properties of the material. This data comprised the direct energy gap, indirect energy gap and optical absorption edge of the material. The direct optical energy gap for pure PVA lies at 6.08 eV, while PVA doped with zinc sulphide ranges from 5.28 to 5.68 eV for the different compositions. It was evident that the energy gaps and band edge values transferred to lower energies on doping with ZnS up to a dopant concentration of 92 wt.% of PVA and 8 wt.% of ZnS. For this study, the ionic conductivity and transference number of PVA polymer electrolytes were measured in order to know more about the conductivity order and charge transport in these materials. The charge transport in PVA polymer electrolyte was measured to be largely due to ions (t_{ion} = 0.97), as indicated by the transference number. Increasing the ZnS concentration and the temperature were both found to raise the ionic conductivity. The discharge properties of solid-state battery cells made with this PVA polymer electrolyte were studied while operating under a constant load of 100 kW.

Keywords: Polymer electrolytes, Polyvinyl alcohol, Ionic conductivity, Discharge characteristics.

INTRODUCTION

Advances in ionic conductivity, mechanical, thermal and electrochemical stability of polymer electrolytes have been the focus of extensive research in recent years. Electrochromic and temperature-sensitive printed electronics devices, solar cells, biomedical sensors, supercapacitors and batteries are just a few examples of the many uses for solid polymer electrolytes [1]. Polyvinyl alcohol (PVA) is well-known for its tremendous impact strength at low temperatures, especially its flexibility, good moldability, high strength, heat-stable and chemical resistance [2,3]. PVA is a high-priority material because of its exceptional flexibility, great corrosion resistance, superior radiation resistance, adherence to different surfaces, and high affinity with alternative polymers [4]. Polyvinyl alcohol is a crucial structure of composites that compete in different applications and industries due to its remarkable specifications. This polymer is generally a resin correlated with applications that demand flexibility, strong binding, toughness and optical clarity [5]. PVA is a remarkable organic component due to its excellent compatibility with inorganic materials. It is extensively used as functional material in diverse fields to fabricate organic/inorganic hybrid composites [6]. Due to the high concentration of hydroxyl groups in PVA, it is soluble in a wide range of organic solvents and can be combined with a wide range of species to improve solvent, chemical and thermal resistances. It also controls adhesion to surfaces, enhances thermoset resin properties, influences crosslinking behaviour and modifies the miscibility and morphology of blends [7].

As an anode in solid-state batteries, zinc is the preferred choice due to its abundant availability from the earth's crust and high performance qualities [8]. The present paper investigates solid polymer electrolyte films of PVA doped with different compositions of zinc sulphide (ZnS) systems. Several techniques such as XRD, FTIR, optical analysis, electrical and transport property measurements were implemented to charact-

erize these polymer electrolytes. Electrochemical cells were fabricated using these polymer electrolytes with the configuration anode/polymer electrolyte/cathode. The properties of electric discharge characteristics of the cell were studied for a load of 100 kW.

EXPERIMENTAL

Films (thickness 80-100 μm) of pure PVA, 98:02 PVA + ZnS, 96:04 PVA + ZnS, 94:06 PVA + ZnS and 92:08 PVA + ZnS (termed as Pure PVA, PVA-2 wt.% ZnS, PVA-4 wt.% ZnS, PVA-6 wt.% ZnS and PVA-8 wt.% ZnS) were prepared with triple distilled water as solvent by using the solution-cast technique. These solutions were stirred for 48 h, cast onto polypropylene dishes and evaporated thoroughly at 60 ºC for 48 h in an air-controlled vacuum oven. The film was then characterized to study the various structural, optical, electrical and discharge studies. The optical studies of pure PVA and PVA complexed with different compositions of ZnS were observed in the wavelength range of 200-1100 nm employing the UV-visible spectrophotometer (Model: Shimadzu UV-800). The XRD analysis of the films was performed with a gracing incidence X-ray diffractometer with Cu*K*α radiation. The FTIR spectra were recorded in the range of 4000-500 cm^{-1} using a FTIR spectrophotometer (Model: Shimadzu FTIR 8400S). The electrical conductivity study was performed as a function of temperature employing a lab-made conductivity cell setup. It was established that the ionic transport number could be measured by using Wagner's polarization approach. The electrochemical cells were fabricated with a configuration Zn/(PVA-8wt.% ZnS)/(I_2 + C + piece of electrolyte) and the discharge properties of these cells were studied for a constant load of 100 kW.

RESULTS AND DISCUSSION

XRD studies: The XRD study for the complexation of (PVA:ZnS) with different ZnS composition (0, 2, 4, 6 and 8 wt.%) is shown in Fig. 1. XRD spectrum of pure PVA has its characteristic peaks obtained at 2θ = ~19.80º, where the peak is moderately broad due to amorphous nature of the polymer. After the addition of ZnS into the PVA matrix, the diffraction peaks of the resulted in composite films shifted to 19.69º, 19.59º, 19.38º and 19.28º for PVA-2 wt.% ZnS, PVA-4 wt.% ZnS, PVA-6 wt.% ZnS and PVA- 8 wt.% ZnS, respectively for PVA+ ZnS electrolyte system. In the XRD patterns of the prepared films, there is a small but sharp ZnS peak at 2θ = 26.56º appeared. The fact that the peak positions of all of the prepared composite films are equivalent, which indicates that ZnS is distributed uniformly throughout the PVA matrix [9]. This is demonstrated by the fact that PVA films with a slightly changed amorphous structure that were strengthened with ZnS were able to be prepared successfully. Due to the presence of multiple hydroxyl groups on its backbone, the structure of the ZnS does not suffer any modifications when it is absorbed into the PVA matrix [10]. Interference between PVA chains and ZnS causes a reduction in the strength of the intermolecular contact that occurs between PVA chains. As a result of these

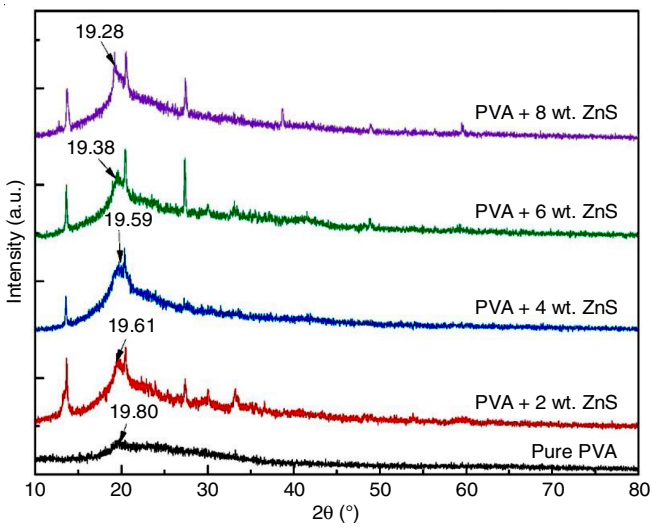

Fig. 1. XRD spectra of pure and ZnS doped PVA films

changes, the amorphous nature of PVA increases together with the weight percent of ZnS. Using Gaussian fitting of the observed XRD peaks (Fig. 1), 2θ, β and D values of the pure and ZnS doped PVA nanocomposite films are given in Table-1. The diffractograms could also make the observation that the intensity of the peak diminishes in direct proportion to the growing amount of ZnS in the prepared nanocomposite films (Fig. 1). The amount of ZnS in the film caused the XRD peaks to become wider as the concentration of ZnS increased.

TABLE-1
BRAGG'S ANGLE (2θ), FULL-WIDTH HALF MAXIMUM (FWHM) (β) AND THE CRYSTALLITE SIZE (D) OF PURE AND ZnS DOPED PVA POLYMER ELECTROLYTE FILMS

Composition	2θ	Intensity	β (rad)	D (nm)
Pure PVA	19.80	288	0.3764	0.3910
PVA-2 wt.% ZnS	19.69	355	0.3400	0.4323
PVA-4 wt.% ZnS	19.59	487	0.2755	1.8733
PVA-6 wt.% ZnS	19.38	1693	0.0165	8.9388
PVA-8 wt.% ZnS	19.28	1790	0.0157	9.3990

Morphological studies: Fig. 2 shows the SEM images of pure PVA and PVA-ZnS nanocomposite films with 2.0, 4.0, 6.0 and 8.0 wt.% of ZnS and the clusters of spherical-shaped particles are observed. In the nanocomposite films of PVA-ZnS, the distribution of particles is uniform throughout the sample. It is also observed that several aggregate particles and pores have reduced due to the uniform distribution of ZnS particles in the PVA-ZnS nanocomposite films. In these nanocomposite films, PVA molecules are interlinked with ZnS particles, which is responsible for the electrical conductivity in nanocomposite films. Fig. 2a shows clearly that the nanoflake structure found in composite micromorphology is made up of numerous nanospheres. When ZnS nanoparticles were introduced, the smooth surface of PVA disappeared, but the particle shape emerged as ZnS concentration increases. All the PVA/ZnS nanocomposite films had a rougher surface compared to pure PVA, proving that the ZnS had been evenly distributed throughout the polymer. The PVA/ZnS composite,

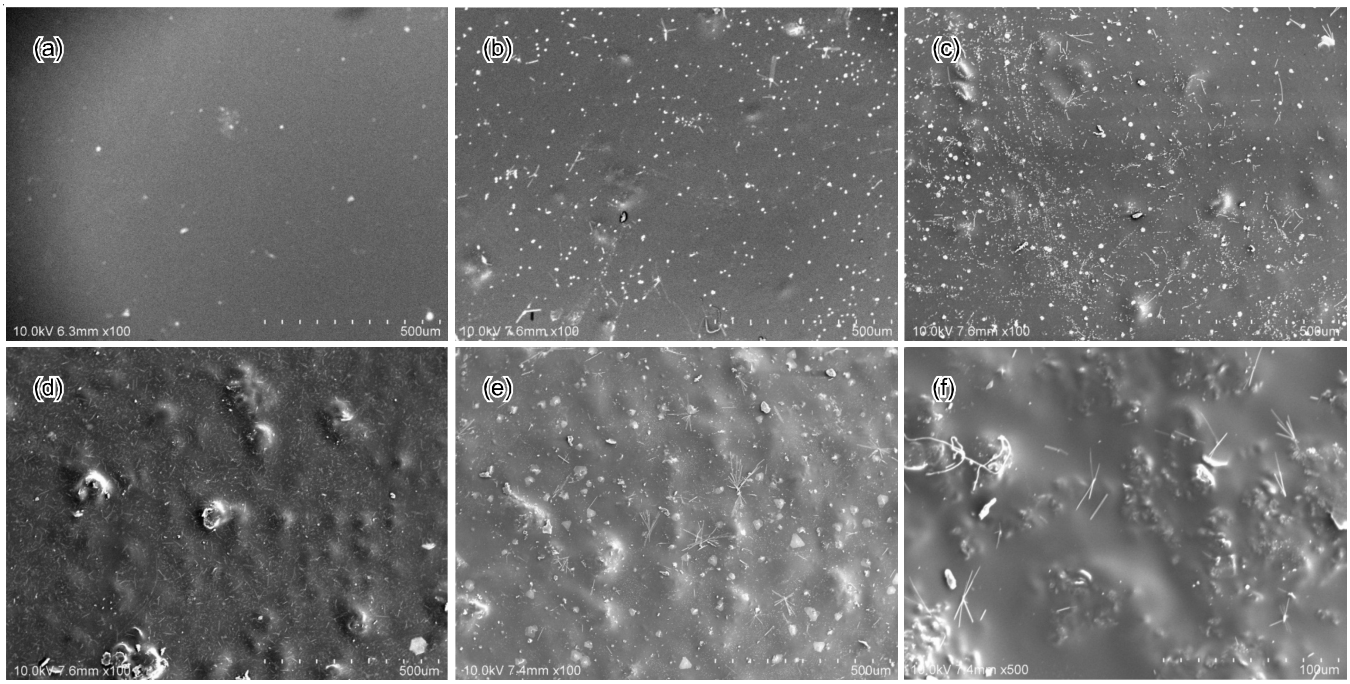

Fig. 2. Surface morphology of (a) pure PVA, (b) PVA-2 wt.% ZnS, (c) PVA-4 wt.% ZnS, (d) PVA-6 wt.% ZnS, (e) PVA-8 wt.% ZnS and (f) PVA-8 wt.% ZnS (agglomerated) nanocomposite films

due to its nanoscale size, is well-suited for use as a functional filler that incorporates the benefits of ZnS.

FTIR studies: An FTIR spectroscopy was used to investigate the complexation in the polymer matrices with changes in the band assignment of the spectra. The FTIR spectra of pure PVA and PVA doped with 2, 4, 6 and 8 wt.% of ZnS are shown in Fig. 3. Several alterations in spectral characteristics were then observed and listed in Table-2 after comparing the spectra of pure PVA and PVA doped with various concentrations of ZnS.

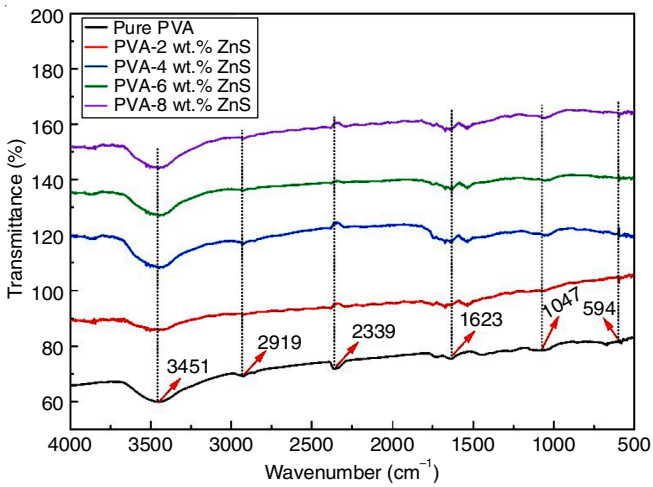

Fig. 3. FTIR spectra of pure and Zn^{2+} ions doped PVA polymer electrolyte films

The peak centred at 3451 cm^{-1} assigned to the stretching vibration of hydroxyl groups (O–H) of pure PVA [11,12] was shifted to 3446, 3445.6, 3445.5 and 3445.2 cm^{-1}, respectively, in 2, 4, 6 and 8 wt.% ZnS in PVA+ ZnS electrolyte system,

TABLE-2
FTIR PEAK ASSIGNMENT OF PVA-8 wt.% ZnS POLYMER NANOCOMPOSITE FILMS

Wavenumber (cm^{-1})	Band assignment
3445.2	O-H stretching vibration
2917.3	Asymmetric stretching of -CH_2
2337.2	O-H bend
1621.3	Unsaturated C = C stretching mode
1046.3	ν(C=O) stretching vibration of the ether group
593.1	Metal sulphide bending

which indicates the specific interaction in the polymer systems. In addition to this, the C–H stretching of CH_2, which showed absorption at 2919 cm^{-1} in pure PVA [11,12], was shifted to 2918.5, 2918.3, 2918.1 and 2917.3 cm^{-1} in 2, 4, 6 and 8 wt.% PVA + ZnS, respectively (Fig. 3). The peak centred at 2339 cm^{-1} assigned to the bending of hydroxyl groups (O–H) of pure PVA [11,12] was shifted to 2338.5, 2338.1, 2337.6 and 2337.2 cm^{-1}, respectively in 2, 4, 6 and 8 wt.% ZnS in PVA + ZnS electrolyte system, which indicates the specific interaction in the polymer systems. The peak at 1623 cm^{-1} corresponding to C=C stretching of PVA [11,12] was shifted to 1622.6, 1622.3, 1621.8 and 1621.3 cm^{-1} in the 2, 4,6 and 8 wt.% ZnS in PVA + ZnS system. The C=O stretching occurred at 1047 cm^{-1} in PVA [11] and was shifted to 1046.5, 1046.4,1046.2 and 1046.3 cm^{-1} in 2, 4, 6 and 8 wt.% ZnS in PVA + ZnS electrolyte systems. This clearly showed that the interaction between the ZnS dopant salt and PVA in the polymer composite does not only arise from O–H group but also from the C–O group of pure PVA. The vibration peak appearing at 594 cm^{-1} assigned to C–H out of plane bend of PVA and also Zn-S bending vibration [11,12] was shifted to 593.7, 593.6, 593.5 and 593.1 cm^{-1}, respectively in 2, 4, 6 and 8 wt.% ZnS in PVA + ZnS complexed electrolyte systems. The proton in the salt interacting with the carbonyl

oxygen of PVA may cause a change in this wave number. Both PVA polymer and ZnS dopant had complexed was demonstrated by the FTIR study.

Optical studies: The optical analysis was used to analyze the optical band gap of the materials with the modifications in electronic transitions of the transmitted radiation. The fundamental absorption, also known as absorption edge, can be used to evaluate the optical band gap ($E_g = hc/\lambda$), where h is Planck's constant. The absorption coefficient (α) was determined by using eqn. 1:

$$\alpha = \frac{2.3032}{d} \times A \quad (1)$$

where A is absorbance and d is the film thickness.

Fig. 4 depicts the optical absorption spectra of pure and PVA polymer films doped with varying amounts of ZnS at ambient temperature, covering the wavelength range of 200-800 nm. The presence of carbonyl groups (C=O) is responsible for the 222 nm absorption edge attributed to the $n \rightarrow \pi^*$ transition. As the number of Zn^{2+} ions per unit volume of PVA polymer increased, the corresponding absorption band moved to longer wavelengths. ZnS has become complexed into the PVA matrix, as evidenced by a shift in higher wavelength and a difference in energy gap (E_g) between pure and ZnS doped films.

Fig. 5 represents the photon's energy *versus* the optical absorption coefficient for pure PVA and PVA doped with different ZnS compositions. The absorption edge is minimum (5.11 eV) for the composition of 92% PVA and 8% ZnS and above this concentration, the absorption edge is shifted to higher energy. It is evident that the absorption edge is high in pure PVA. With the increase in ZnS concentration into the PVA matrix, the absorption edge is shifted to photon energy range from 5.82 eV to 5.11 eV representing a decrease of the bandgap with the addition of Zn^+ ions into the PVA matrix.

Energy band gap: In optical absorption study, the electronic band structure of solids can be determined to study the range of energy levels of the electrons. The transition in bandgap energy can determine the optical bandgap energies, such as direct and

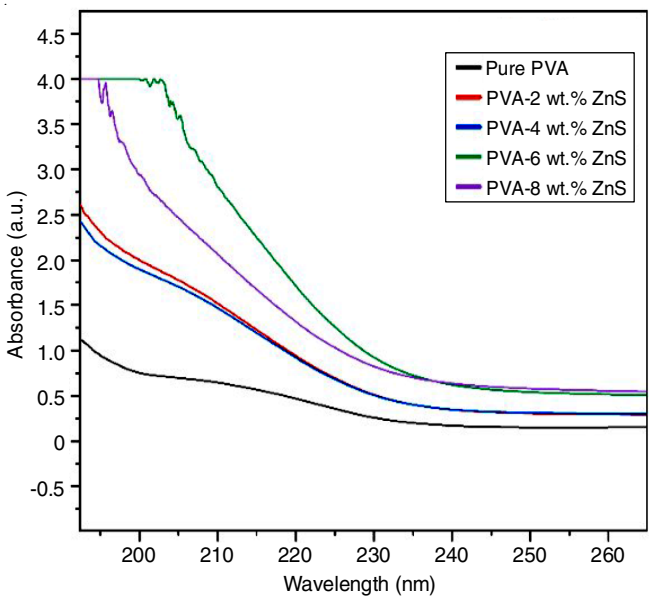

Fig. 4. UV-visible absorption spectra of pure and Zn^{2+} ions doped PVA polymer electrolyte films

indirect band gaps. Both the conduction and valence bands coexist in the direct band at zero crystal momentum. Indirect bandgap transitions occur between the valence and conduction bands, and are linked to the phonon associated with the crystal's momentum magnitude [13]. Davis & Shalliday [14] observed that a plot of $(\alpha h\nu)^{1/2}$ and $(\alpha h\nu)^2$ as a function of photon energy may account for the simultaneous development of indirect and direct energy bandgaps close to the fundamental band edge. The photon energy ($\alpha h\nu$) *versus* the photon frequency ($h\nu$) graph as illustrated in Fig. 6 can be used to calculate the absorption bandgap and Table-3 displays the values for the energy band gaps. Fig. 7 shows the band gap for the permitted direct transition ($x = 2$), whereas Fig. 8 shows the band gap for the forbidden indirect transition ($x = 1/2$). Using ($h\nu$) photon energy, one may calculate the absorption coefficient, absorption edge, and valence-to-conduction band energy gap of an electron.

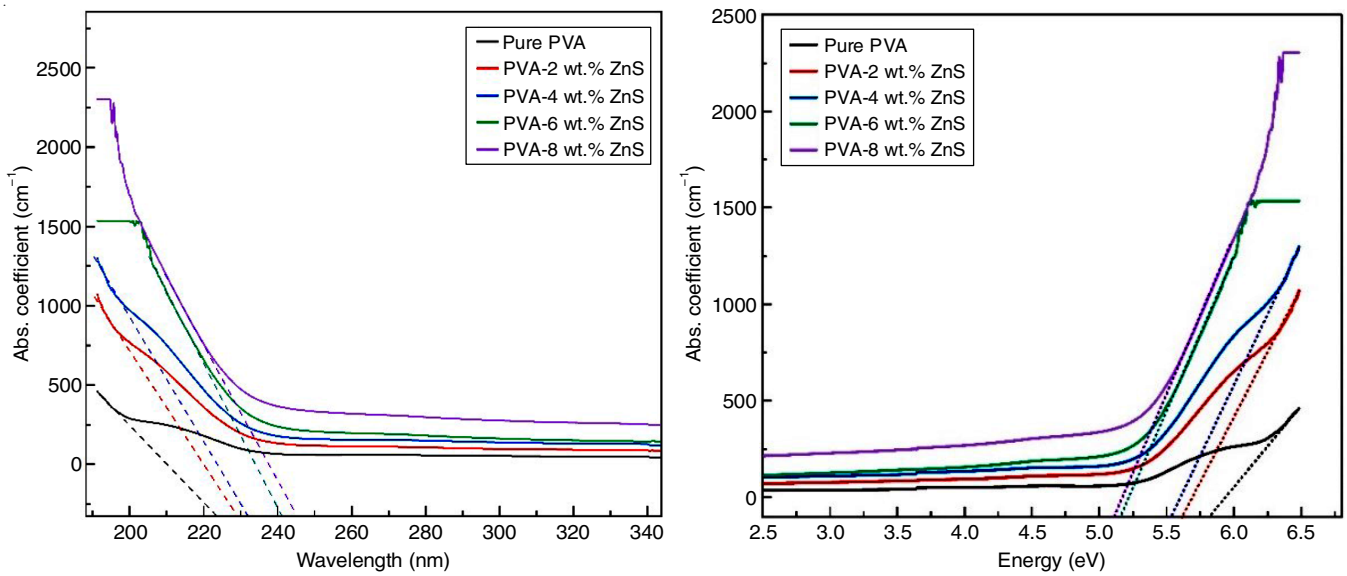

Fig. 5. α *vs.* λ and α *vs.* $h\nu$ curves of pure and Zn^{2+} ions doped PVA polymer electrolyte films

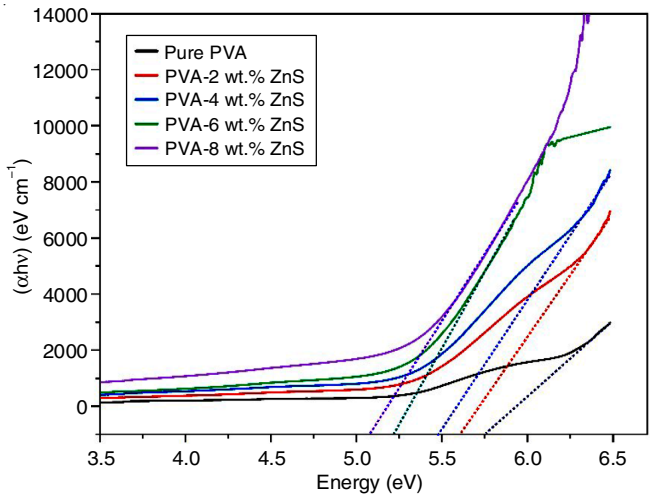

Fig. 6. αhν *vs.* hν curves of pure and Zn^{2+} ions doped PVA polymer electrolyte films

TABLE-3
VALUES OF ABSORPTION EDGE, DIRECT BANDGAP AND INDIRECT BANDGAP OF PURE AND Zn^{2+} IONS DOPED PVA POLYMER ELECTROLYTE FILMS

Composition	Absorption edge (nm)	Direct bandgap	Indirect bandgap
Pure PVA	222	6.09	5.53
PVA-2 wt.% ZnS	228	5.68	4.76
PVA-4 wt.% ZnS	231	5.35	4.66
PVA-6 wt.% ZnS	240	5.33	4.73
PVA-8 wt.% ZnS	245	5.28	4.64

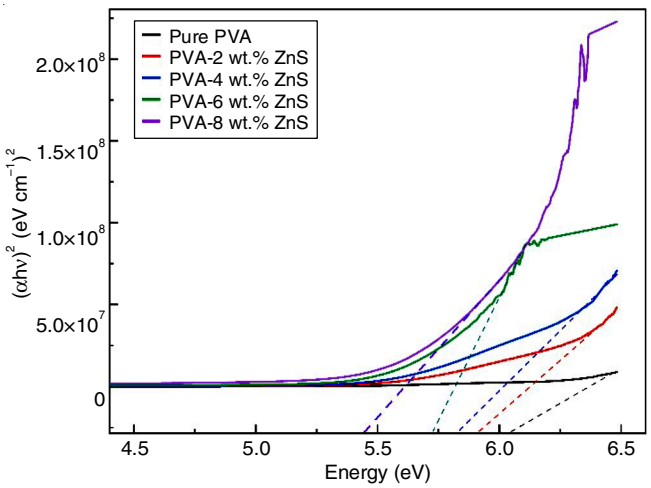

Fig. 7. $(\alpha h\nu)^2$ *vs.* hν curves of pure and Zn^{2+} ions doped PVA polymer electrolyte films

In present work, a direct bandgap of 6.09 eV and an indirect band gap of 5.53 eV is obtained for pure PVA. The direct and indirect bandgap shifted to different energy with the addition of Zn^{2+} ions. It reached a minimum value for all the band gaps energy up to 92% of PVA and 8% of ZnS concentration.

DC Conductivity studies: Study into DC conductivity provides the most apparent proof for the benefits of using solid polymer electrolytes in certain electrochemical device applications [15]. The conductivity was measured by using the DC polarization technique at different temperatures with an increasing temperature range of 303-377 K. Based on Ohm's law, the ionic conductivity can be represented as:

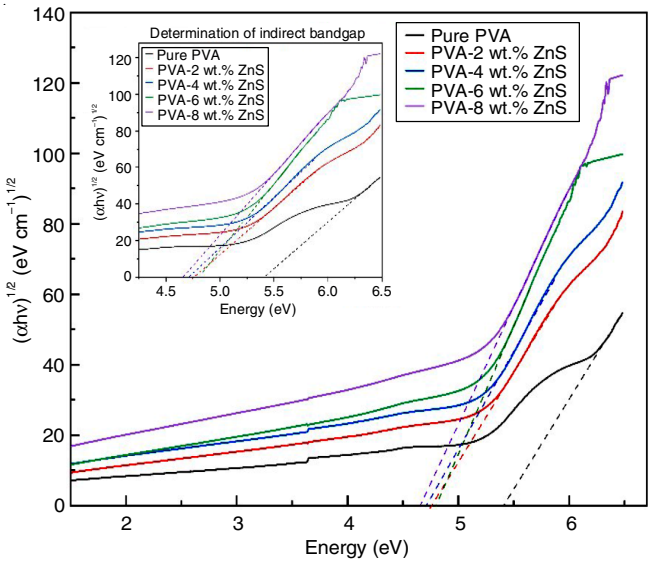

Fig. 8. $(\alpha h\nu)^{1/2}$ *vs.* hν curves of pure and Zn^{2+} ions doped PVA polymer electrolyte films

$$\sigma = \frac{t}{RA} \qquad (2)$$

where V is the applied potential, I is the current, t is the sample thickness and A is the area of the cross-section of the sample specimen. The ionic conductivity of PVA polymer electrolytes as a function of ZnS concentration at different temperatures is shown in Fig. 9. According to the obtained results (Table-4), for PVA-2 wt.% ZnS prepared nanocomposite films provide the excellent thermal conductivity of about 1.874×10^{-12} S/cm at room temperature and 9.424×10^{-11} S/cm at 373 K, which increases with the addition of ZnS content till a maximum conductivity of about 9.424×10^{-11} S/cm at room temperature and 8.516×10^{-8} S/cm at 373 K for PVA-8 wt.% ZnS. It can be observed that the conductivity increases as the salt content increases up to 8 wt.%, which can be attributed to the enhancement of the ionic conductivity resulting from increased ionic mobility and ionic charge carrier concentration. The high amorphousness of the polymer electrolyte sheets increases the conductivity since it increases the mobility of the charge carrier. There is a one-to-one relationship between the mobility and number of charge carriers and the conductivity of the polymer electrolytes [16]. The plot shows that the ionic conductivity increases with the temperature increment, which may be due to increased chain flexibility and decreased viscosity [17]. The activation energy values were calculated from Fig. 9, using the following Arrhenius equation:

$$\sigma = \sigma_o \exp\left(\frac{-E_a}{kT}\right) \qquad (3)$$

where σ_o is a constant, E_a is the activation energy, k is the Boltzmann constant and T is the absolute temperature. The activation energy values were 0.27, 0.22, 0.15, 0.14 and 0.13 eV for pure and 2, 4, 6 and 8 wt.% PVA-ZnS nanocomposite films, respectively. When ZnS is incorporated into the PVA

TABLE-4
CONDUCTIVITY, ACTIVATION ENERGY AND IONIC TRANSFERENCE NUMBER VALUES OF PURE AND ZnS INCORPORATED PVA POLYMER ELECTROLYTE FILMS

Polymer electrolyte composition	Ionic conductivity		Activation energy (eV)	Transference number	
	303 K	373 K		t_{ion}	t_{elec}
Pure PVA	5.569×10^{-13}	8.608×10^{-12}	0.2744	–	–
PVA-2 wt.% ZnS	1.874×10^{-12}	3.384×10^{-10}	0.2213	0.9410	0.0589
PVA-4 wt.% ZnS	1.194×10^{-11}	1.916×10^{-9}	0.1515	0.9687	0.0312
PVA-6 wt.% ZnS	2.973×10^{-11}	1.034×10^{-8}	0.1496	0.9755	0.0201
PVA-8 wt.% ZnS	0.942×10^{-10}	0.851×10^{-7}	0.1390	0.9788	0.0211

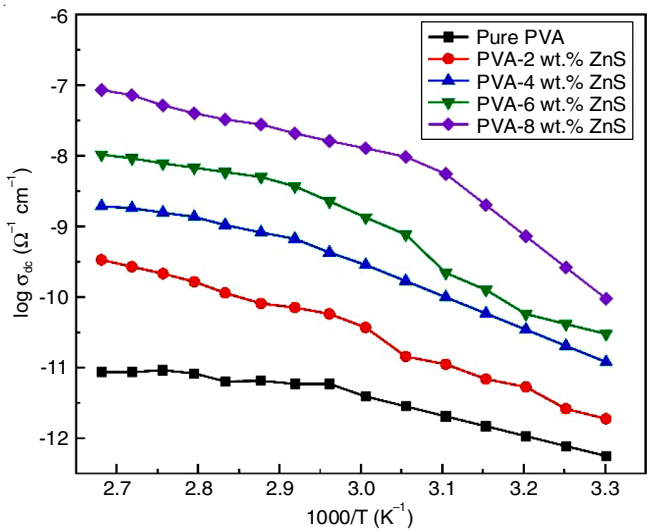

Fig. 9. Plot of log σ_{dc} *vs.* 1000/T of pure and Zn^{2+} ions doped PVA polymer electrolyte films

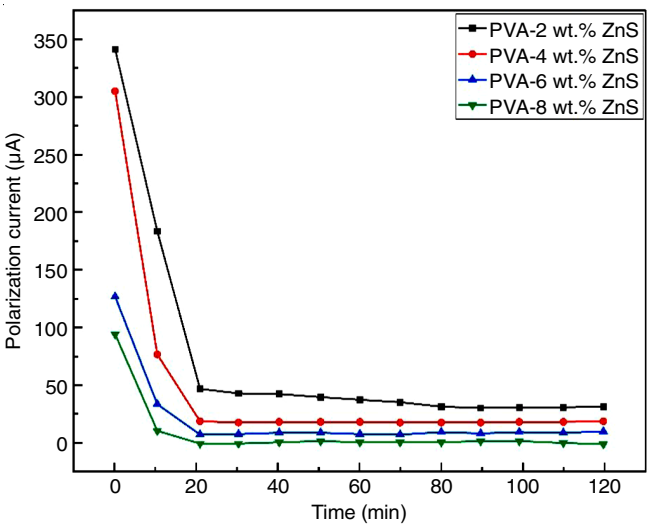

Fig. 10. Ionic transference number of pure and Zn^{2+} ions doped PVA polymer electrolyte films at room temperature

matrix, the activation energy decreases since the amorphous structure of the PVA polymer electrolyte allows for rapid Zn^{2+} ion mobility inside the polymer network.

Transport properties: It is important to take into account about transference numbers and ionic conductivities while developing a new polymer electrolyte for batteries. The transference number is measured to determine whether the sample's conductivity is predominantly due to ions or electrons. The ionic transference number in the polymer electrolyte was calculated using Wagner's DC polarization method [18]. The total conductivity of a solid polymer electrolyte is calculated by adding the ionic and electronic conductivities.

Wagner's polarization method is used to measure the ionic transference numbers. It denotes the fraction of current carried by anions and cations or electrons in the material in terms of total conductivity. The fraction of the conductivity due to ions or electrons is given by:

$$t_{ion} = \frac{\sigma_{ion}}{\sigma_T} \quad (4)$$

$$t_{elec} = \frac{\sigma_{ele}}{\sigma_T} \quad (5)$$

where t_{ion} and t_{ele} are referred to as the ionic and electronic transference numbers, respectively, whereas σ_{ion}, σ_{ele} and σ_{tot} are conductivity due to ions, electrons and total conductivity, respectively. In this method, silver electrodes/polymer electrolyte/silver electrodes were used to polarize the produced films under a DC bias (step potential 2 V). After the electrolyte was polarized, the current was recorded over time. The transport number was calculated from the initial current, I_i and final residual current, I_f using the formulae $I_f = I_{ion} + I_{ele}$. The polarization current *vs.* time plot at room temperature is obtained, which is given in Fig. 10. From the graph, a large value of initial current (μA) is established due to the involvement of electrons, cations and anions [19] and a sudden drop in current is observed with the function of time, which indicates that the samples are ionically conducting species [20]. The current through the circuit was monitored until it reaches saturation at ambient temperature. The measured transference number values are given in Table-4. In these polymer electrolyte systems, the total ionic transference number was found to be in the range of 0.9410-0.9788, which suggests that the charge transport in these polymer electrolytes is predominantly due to the ions.

Discharge characteristics: In present studies, the cathode material is composed of three distinct elements, including an active cathode, particles of an electronic conductor (such as carbon) and the surrounding polymer electrolyte material [21]. The preference for choosing anode material in a solid-state battery depends on the mobile species in the electrolyte [22]. Zinc metal was used as the positive electrode and a mixture of iodine (I_2), carbon (C) and a piece of electrolyte in the ratio of 5:5:1 as the negative electrode. It was found that solid-state electrochemical cells may be constructed using Zn/PVA + ZnS/(I_2 + C + piece of electrolyte) polymer electrolyte sheets. Using

PVA + ZnS polymer electrolyte films, solid-state electrochemical cells were fabricated with the configuration Zn/PVA + ZnS/(I_2 + C + piece of electrolyte). The observed discharge characteristic for 92:08::PVA:ZnS is shown in Fig. 11. The discharge characteristics of the cells Zn/(PVA + ZnS) (92:08)/(I_2 + C + piece of electrolyte) at ambient temperature were calculated and the values are given in Table-5.

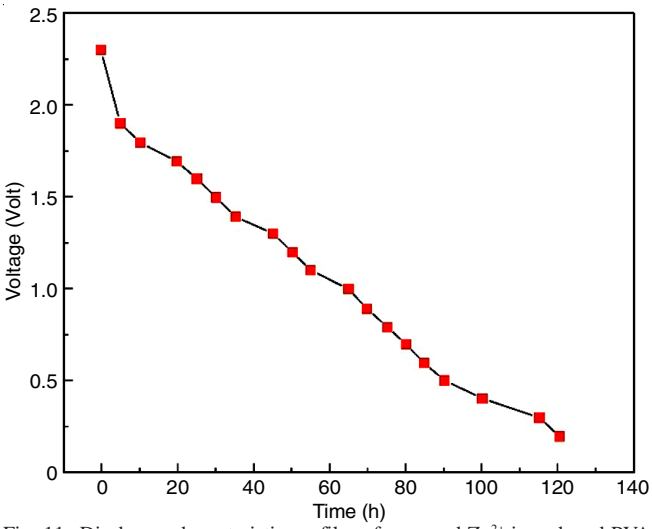

Fig. 11. Discharge characteristic profiles of pure and Zn^{2+} ions doped PVA polymer electrolyte films

TABLE-5
DISCHARGE CHARACTERISTICS OF THE CELLS Zn/(PVA + ZnS) (92:08)/(I_2 + C + PIECE OF ELECTROLYTE) AT AMBIENT TEMPERATURE

Cell parameters	
Area of the electrolyte (cm^2)	1.1
Cell weight (g)	1.5
Open circuit voltage (V)	2.3
Short circuit current (μA)	1.3
Discharge time for plateau region (h)	90
The density of power (W/Kg)	2.990
The density of energy (Wh/Kg)	269.1
Current density (A/cm^2)	1.1818
Capacity of discharge (μA h^{-1})	14.4

Conclusion

Using a solution casting method, polyvinyl alcohol (PVA) based electrolytes doped with Zn^{2+} ions of varying concentrations were developed. The shorter crystallite length D was observed in the X-ray diffraction patterns, which suggested that the polymer electrolyte becomes more amorphous as dopant concentration increases. The FTIR spectra of the prepared samples showed that the intensity and position of some bands changed, indicating that Zn^{2+} ions were complexed with the host polymer. The optical analysis indicates that with increasing dopant concentration in the PVA polymer matrix, the optical band gap (both direct and indirect) shifted to the lower energy. The ionic conductivity was found to be increasing due to the increased concentration of Zn^{2+} ions. The maximum ionic conductivity of 5.62×10^{-7} S cm^{-1} at 303 K has been observed for 8 wt.% Zn^{2+} ions doped PVA based electrolyte sample, which indicates an increase in the amorphous character of the polymer electrolyte. The transference number indicated that the conduction in these polymer electrolytes was predominantly due to ions rather than electrons. The open circuit voltage (OCV) and short circuit current (SCC) of electrochemical cells fabricated with (92 PVA: 08 ZnS) electrolyte composite films were found to be 2.3 V and 1.3 mA, respectively. The evaluated cell parameters of the cell (Zn/92 PVA:08 ZnS)/(I_2 + C + electrolyte)) offer a significant application for solid-state batteries. Hence, the analyzed properties of Zn^{2+} ions doped with PVA polymer electrolytes are highly acceptable and promising for battery applications.

CONFLICT OF INTEREST

The authors declare that there is no conflict of interests regarding the publication of this article.

REFERENCES

1. D. Golodnitsky, E. Strauss, E. Peled and S. Greenbaum, *J. Electrochem. Soc.*, **162**, A2551 (2015); https://doi.org/10.1149/2.0161514jes
2. J.C. Hoepfner, M.R. Loos and S.H. Pezzin, *J. Appl. Polym. Sci.*, **135**, 46157 (2018); https://doi.org/10.1002/app.46157
3. K. Nakane, T. Kurita, T. Ogihara and N. Ogata, *Compos., Part B Eng.*, **35**, 219 (2004); https://doi.org/10.1016/S1359-8368(03)00066-0
4. R.M. Omer, E.T.B. Al-Tikrity and N. Rasheed, *Prog. Color Colorants Coat.*, **15**, 191 (2022); https://doi.org/10.30509/PCCC.2021.166839.1120
5. A. Rajeshwar Reddy, Ch. Srinivas and N. Narsimlu, *Mater. Today Proc.*, **67**, 912 (2022); https://doi.org/10.1016/j.matpr.2022.07.391
6. L.-J. Chen, J.-D. Liao, S.-J. Lin, Y.-J. Chuang and Y.-S. Fu, *Polymer*, **50**, 3516 (2009); https://doi.org/10.1016/j.polymer.2009.05.063
7. Z.W. Abdullah, Y. Dong, I.J. Davies and S. Barbhuiya, *Polym.-Plast. Technol. Eng.*, **56**, 1307 (2017); https://doi.org/10.1080/03602559.2016.1275684
8. K. Singh, Y. Yao, T. Ichikawa, A. Jain and R. Singh, *Batteries*, **8**, 113 (2022); https://doi.org/10.3390/batteries8090113
9. A. Arya and A.L. Sharma, *Ionics*, **23**, 497 (2017); https://doi.org/10.1007/s11581-016-1908-6
10. P. Kumar, N. Khan and D. Kumar, *Green Chem. Technol. Lett.*, **2**, 185 (2016); https://doi.org/10.18510/gctl.2016.244
11. O. Olabisi and K. Adewale, Polyvinyl Butyral, In: Handbook of Thermoplastics, CRC Press (2015).
12. F. Lian, Y. Wen, Y. Ren and H.Y. Guan, *J. Membr. Sci.*, **456**, 42 (2014); https://doi.org/10.1016/j.memsci.2014.01.010
13. S.B. Aziz, T.J. Woo, M.F.Z. Kadir and H.M. Ahmed, *J. Sci. Adv. Mater. Devices*, **3**, 1 (2018); https://doi.org/10.1016/j.jsamd.2018.01.002
14. P.W. Davis and T.S. Shilliday, *Phys. Rev.*, **118**, 1020 (1960); https://doi.org/10.1103/PhysRev.118.1020
15. N. Krishna Jyothi, K. Vijaya Kumar and P. Narayana Murthy, *Int. J. ChemTech. Res.*, **6**, 5214 (2014).
16. S. Ramesh, A.H. Yahaya and A.K. Arof, *Solid State Ion.*, **152-153**, 291 (2002); https://doi.org/10.1016/S0167-2738(02)00311-9
17. J.M. Hadi, S.B. Aziz, S. R. Saeed, M.A. Brza, R.T. Abdulwahid, M.H. Hamsan, R. M. Abdullah, M.F.Z. Kadir and S.K. Muzakir, *Membranes*, **10**, 363 (2020); https://doi.org/10.3390/membranes10110363
18. D. Ghosh, G. Ahamed, S. Batuta, N.A. Begum and D. Mandal, *J. Phys. Chem. A*, **120**, 44 (2016); https://doi.org/10.1021/acs.jpca.5b09681
19. J.B. Wagner and C.J. Wagner, *J. Chem. Phys.*, **26**, 1597 (1957); https://doi.org/10.1063/1.1743590
20. J.C. Hoepfner, M.R. Loos and S.H. Pezzin, *J. Appl. Polym. Sci.*, **135**, 46157 (2018); https://doi.org/10.1002/app.46157
21. S.K.S. Basha, G.S. Sundari, K.V. Kumar and M.C. Rao, *Polym. Sci. Ser. A*, **59**, 554 (2017); https://doi.org/10.1134/S0965545X17040095
22. B. Bhargav, V.M. Mohan, A.K. Sharma and V.V.R.N. Rao, *Curr. Appl. Phys.*, **9**, 165 (2009); https://doi.org/10.1016/j.cap.2008.01.006